Solar Phys (2007) 242: 43–52
DOI 10.1007/s11207-007-0344-1

Prominences on the Limb: Diagnostics with UV – EUV Lines and the Soft X-Ray Continuum

U. Anzer · P. Heinzel · F. Fárnik

Received: 31 October 2006 / Accepted: 8 May 2007 /
Published online: 14 June 2007

Abstract In this paper we discuss the two mechanisms by which solar prominences on the limb can manifest themselves when observed in coronal UV – EUV lines and in the soft X-ray continuum. These mechanisms are the absorption in the resonance continua of hydrogen and helium on one hand and the reduction of the emissivity in a part of the coronal volume occupied by a prominence on the other one. We briefly describe earlier observations made with SOHO/SUMER, EIT and *Yohkoh*/SXT. We then discuss how the instruments on the new Japanese satellite *Hinode* can be used for more detailed studies of prominences. We also propose some combined observations between the *Hinode* satellite and the SOHO/SUMER instrument.

1. Introduction

Prominences observed on the solar limb in UV – EUV lines at high temperatures can either be seen in emission or they appear dark relative to the coronal background (or barely visible). In X-rays they will always be dark. Prominences in emission will only be seen for transition region lines that allow the diagnostics of the prominence – corona transition region (PCTR). Such studies have been performed by Engvold *et al.* (1987) and Del Zanna, Chiuderi, and Parenti (2004). But for all lines with a formation temperature of one million degrees or more, the cool prominence and the PCTR do not emit any radiation. The same is the case for the X-ray part of the spectrum. Under these circumstances the only effects the prominence has on the radiation are the absorption of the coronal emission from behind it and the *emissivity blocking*, called *volume blocking* in our earlier work (Heinzel, Anzer, and Schmieder, 2003), of a certain fraction of the coronal volume. Here the term blocking means that a certain

U. Anzer (✉) · P. Heinzel
Max-Planck-Institut für Astrophysik, Karl-Schwarzschild-Str. 1, 85740, Garching, Germany
e-mail: ula@mpa-garching.mpg.de

P. Heinzel · F. Fárnik
Astronomical Institute, Academy of Sciences of the Czech Republic, 25165, Ondřejov, Czech Republic

coronal region is occupied by rather cool plasma and therefore the coronal gas is absent from that part. A similar behavior is found if the region contains a hot plasma with a very low density (*e.g.*, in a coronal void). In both cases coronal line radiation is either absent or negligible from that part of the corona. Both the absorption and the *emissivity blocking* can contribute to the observed darkening. For more details see Anzer and Heinzel (2005).

Depending on the strength of the absorption and the extension of the blocking region along the line of sight the amount of darkening can range from almost invisible to intensity reductions of 50%, or even more. As discussed by Anzer and Heinzel (2005) the absorption of the EUV line radiation is due to the continua of H I, He I, and He II. But for those lines that lie above the head of the Lyman continuum of hydrogen at 912 Å no significant absorption will take place. The absorption from the C I continuum discussed by Foukal (1981) is several orders of magnitude too small for typical prominence conditions.

Soft X-rays with wavelengths around 50 Å, or lower, can be absorbed by the continua of hydrogen and helium, but the cross sections are so small that the effect will be completely negligible (Heinzel *et al.*, 2007). Therefore the soft X-rays can be used for prominence diagnostics in a similar way as those UV lines that lie above 912 Å.

Since the new satellite *Hinode* will have observing capabilities both in coronal EUV lines and also in the soft X-ray region the observations could be used for a new, detailed modeling of limb prominences. In a previous study by Heinzel *et al.* (2007), which was based upon a combination of SOHO (EIT and SUMER/CDS) observations and SXT data from *Yohkoh,* we have performed such a preliminary investigation and shown its diagnostic capability. In Section 2 we briefly summarize the effects that solar prominences can have on the observed coronal radiation. Section 3 gives estimates for absorption cross sections at different wave lengths. In Section 4 we refer to the earlier results obtained from SOHO/Sumer and EIT, and from *Yohkoh*/SXT. Section 5 gives the relevant characteristics of the *Hinode* instruments, and in Section 6 we discuss the expected diagnostic capabilities of the new observations.

2. Absorption and Emissivity Blocking

The mechanisms of absorption and emissivity blocking by cool prominences located at the solar limb have been described in detail by Heinzel *et al.* (2007). They investigated the case where some coronal lines lie above the Lyman continuum limit at 912 Å and some others below it. For all lines above 912 Å the prominence is basically transparent and only emissivity blocking will occur. Soft X-rays have a similar behavior, as will be discussed in more detail in the next section.

We shall now describe the effect of emissivity blocking. We denote by I the intensity at the position of the prominence and by I_c that of the ambient corona. In the absence of absorption the ratio I/I_c gives the strength of the blocking. For simplicity we have assumed in Heinzel, Dammasch, and Anzer (in preparation) that the prominence is symmetric with respect to the plane of the sky. If the corona is spherically symmetric with an intensity scale height H then the blocking can be approximated by

$$\frac{I}{I_c} = 1 - \frac{L}{L_0}, \tag{1}$$

here L is the blocking length and $L_0 = \sqrt{2\pi R_\odot H}$ determines the length for the coronal emission. This equation holds only if L is sufficiently small compared to the length L_0. If, for example, H is 40 000 km one obtains $L_0 = 420\,000$ km, and therefore only extended structures will give a measurable blocking signal.

Including now the effect of the absorption by cool prominence plasma we obtain the following equation for the total intensity reduction:

$$\frac{I}{I_c} = \frac{1}{2}\left(1 + e^{-\tau}\right)\left(1 - \frac{L}{L_0}\right). \tag{2}$$

Note that the factor $1/2$ arises from our assumption that the prominence and the corona are symmetric with respect to the plane of the sky. The generalization for a small displacement away from the plane of the sky is straightforward but will not be considered here. The other point to notice is the fact that the quantity L_0 is a function of H; therefore if the scale heights for different lines (or of the X-ray continuum and some line) are different then also L_0 and thus the derived blocking effect will be different. But the observations indicate that the scale heights are not drastically different (see the discussion in Heinzel, Anzer, and Schmieder, 2003). Therefore we take as a first approximation a unique value for L_0.

Equation (2) shows that there are the two unknown quantities: τ and L. Therefore if we have observations in two lines with sufficiently different opacities then τ and L can be calculated. We expect that the special case with $\tau = 0$ for one of the lines, or also for the X-rays, and a considerable τ for the other line is particularly useful. On this basis one can then construct prominence models.

3. Estimates for the Absorption Cross Sections

The absorption cross sections in the continua of H I, He I, and He II at the wavelengths of the EUV iron lines 171 Å, 195 Å, and 284 Å have been calculated by Anzer and Heinzel (2005). These calculations can easily be extended to the soft X-ray spectral range. As a typical wavelength we take here 50 Å. (For all shorter wavelengths the cross sections become even smaller.) Since the cross sections of H I and He II scale as λ^3, we refer to the results of Anzer and Heinzel (2005) and can write

$$\sigma_{50} = \sigma_{171}\left(\frac{50}{171}\right)^3 \frac{g(50)}{g(171)}, \tag{3}$$

where g is the Gaunt factor. The cross section of He I is calculated by the numerical approximation given in Rumph, Bowyer, and Vennes (1994); see also Anzer and Heinzel (2005). The approximation is valid down to wavelengths of at least 50 Å. On this basis we determined the following cross sections at 50 Å:

$$\begin{aligned} &\sigma_{\mathrm{H\,I}} = 1.30 \times 10^{-21}\ \mathrm{cm}^2, \qquad \sigma_{\mathrm{He\,I}} = 3.38 \times 10^{-20}\ \mathrm{cm}^2, \quad \text{and} \\ &\sigma_{\mathrm{He\,II}} = 2.08 \times 10^{-20}\ \mathrm{cm}^2. \end{aligned} \tag{4}$$

If we now take a mixture of 90% hydrogen and 10% helium then the optical thickness at 50 Å is given by

$$\tau_{50} = N_{\mathrm{H}}\left\{(1-i)\sigma_{\mathrm{H\,I}} + 0.1\left[(1-j)\sigma_{\mathrm{He\,I}} + j\sigma_{\mathrm{He\,II}}\right]\right\}, \tag{5}$$

where N_{H} is the hydrogen column density, i is the ionization degree of hydrogen, and j is the degree of the first ionization stage of helium. Here we have assumed that doubly ionized

helium can be neglected in prominences. Inserting the values for the cross sections we finally arrive at

$$\tau_{50} = N_{\rm H}(4.68 - 1.30i - 1.30j) \times 10^{-21}. \tag{6}$$

As can be seen from this equation an upper limit on the optical depth is obtained by setting $i = 0$ and $j = 0$. In this case one has

$$\tau_{50} = N_{\rm H} \times 4.68 \times 10^{-21}. \tag{7}$$

For typical prominences we have $N_{\rm H} = 10^{19}$ cm^{-2} (corresponding to a column mass of 2×10^{-5} g cm^{-2}). This leads to

$$\tau_{50} \approx 0.05. \tag{8}$$

This clearly shows that prominences are in general transparent in soft X-rays; only the most extreme cases with column densities larger than 10^{20} cm^{-2} will produce some absorption signal.

The absorption of EUV lines that lie in the wavelength range between 504 and 912 Å is due to the hydrogen Lyman continuum alone. At the head of the Lyman continuum we have $\sigma_{912} = 6.33 \times 10^{-18}$ cm^2; and for $\lambda = 600$ Å we get $\sigma_{600} = 2.23 \times 10^{-18}$ cm^2. This means that in this wavelength range the absorption cross section is at least a factor 45 larger than that for the soft X-rays. Therefore all EUV lines lying around these wavelengths can be strongly absorbed by the prominence plasma (see, Kucera, Andretta, and Poland, 1998; Heinzel *et al.*, 2007; and Anzer and Heinzel, 2003).

We summarize the relative importance of the absorption mechanism at different wavelengths in Table 1. Here the ratios $x = \tau/\tau_{912}$ are given for a plasma with 10% helium, $i = 0.5$, and $j = 0.3$. In Table 1 we further give the values of τ relevant to a central dark part of the 5 September 1996, prominence, computed from τ at 625 Å.

For all lines that lie above the head of the Lyman continuum the most efficient absorbers are probably the continua of C I. For one particular line at 977 Å Foukal (1981) gives a C I continuum cross section of $\sigma_{977} = 3.5 \times 10^{-17}$ cm^2. Taking a carbon abundance ratio of 3×10^{-4} one calculates an efficient cross section (per hydrogen atom) of C I continuum absorption of

$$\sigma_{\rm eff} = 1.2 \times 10^{-20}\ {\rm cm}^2, \tag{9}$$

under the assumption that all the carbon is neutral and in the state from which this particular C I photoionization occurs. In more realistic cases with ionization degrees of 0.5 to 0.8 we get

$$\sigma_{\rm eff} = (2.5 - 6.0) \times 10^{-21}\ {\rm cm}^2. \tag{10}$$

These values are quite similar to the ones we have calculated for the soft X-rays. This implies that the lines in this range will also be rather transparent, unless the density of the structures

Table 1 Theoretical ratio $x = \tau/\tau_{912}$ and the optical thickness τ derived for a central dark part of the 5 September 1996, prominence.

λ [Å]	912	625	284	195	171	50
x	1.0	3.62×10^{-1}	9.43×10^{-2}	4.88×10^{-2}	3.54×10^{-2}	1.15×10^{-3}
τ	7.5	2.7	0.71	0.37	0.27	8.6×10^{-3}

is one to two orders of magnitude larger. Coronal darkening in lines above 912 Å can thus be explained only by the emissivity blocking. In the following we use for our analysis the Fe XII line at 1242 Å observed by SOHO/SUMER. This line lies just above the head of another C I continuum (at 1239 Å) and thus we expect even lower opacity than in the case described by Foukal (1981). However, it would be quite useful to perform detailed non-LTE transfer calculations to obtain the actual opacities in this wavelength range above 912 Å.

4. SOHO and *Yohkoh* Observations

4.1. SOHO/SUMER Observations of Prominences

The limb prominence observed on 5 September 1996, is shown in Figure 1 in four SUMER rasters, which correspond to four lines. S II (1250 Å) and N V (1238 Å) are lower temperature transition-region lines and the prominence appears bright on a dark coronal background. In contrast, in the two coronal lines Mg X (624 Å) and Fe XII (1242 Å) the prominence is dark relative to the bright corona. Similar examples can be found in the SUMER Atlas published by ESA as its special volume SP-1274 (see Feldman *et al.*, 2003).

The mechanisms described in the previous sections are well demonstrated in Figure 2. The Mg X line shows a very dark feature similar in shape to the cool structure visible in the S II line. This is due to hydrogen Lyman-continuum absorption. The much more extended and less dark structure is similar in both Mg X and Fe XII lines. However, in Fe XII we cannot

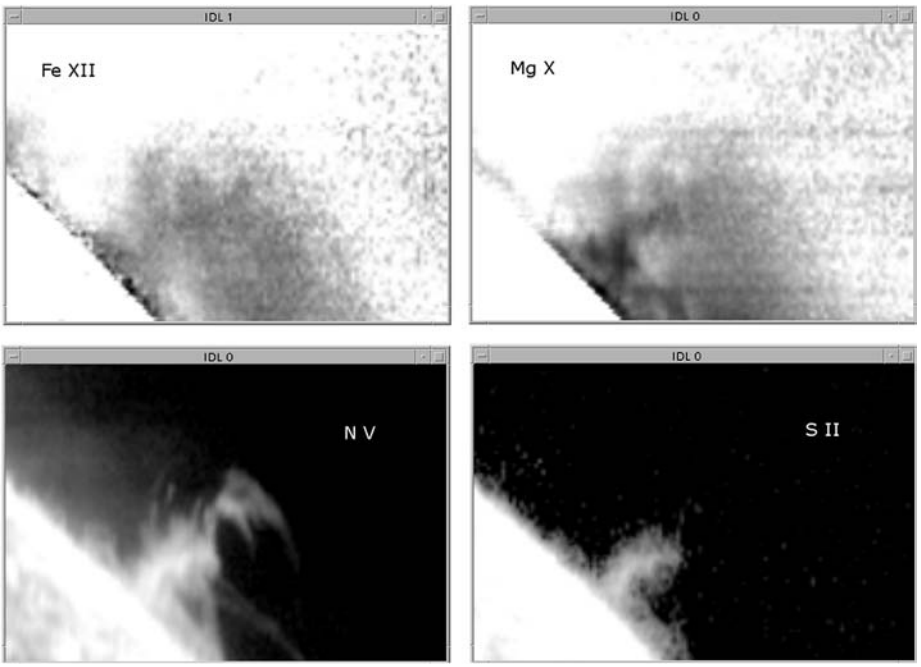

Figure 1 SOHO/SUMER images of the 5 September 1996, prominence. The rasters in four lines of Fe XII (1242 Å), Mg X (624 Å), N V (1238 Å), and S II (1250 Å) are shown. In the Fe XII and Mg X lines we clearly see a lowering of the coronal brightness at the location of the prominence.

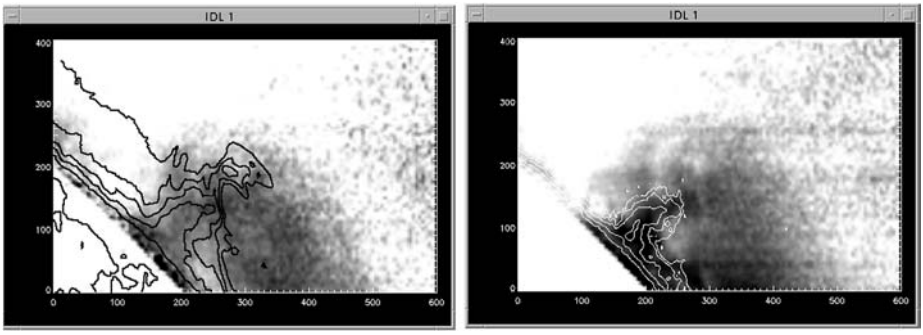

Figure 2 An overlay of the N V image (contours) over the Fe XII image (left) and an overlay of the S II image (contours) over the Mg X image (right).

expect any significant absorption because this line lies above the Lyman-continuum head. So this coronal line clearly shows the importance of emissivity blocking. Using Equation (2) for these two lines, one can discriminate between the absorption and blocking quantitatively. To derive the actual optical thickness at a central location of the dark prominence at the Mg X wavelength, we measured the contrasts from the Mg X and Fe XII images and got the values 0.39 and 0.73, respectively. Assuming no absorption at the Fe XII wavelength, we obtained, using Equations (1) and (2), the value of the optical thickness of the hydrogen Lyman continuum at the position of the Mg X line amounting to 2.7. Based upon this result we can estimate τ at other wavelengths. With this we get τ at 912 Å and then using the ratios x we compute the other τ values (see Table 1).

4.2. SOHO/EIT Images

In Figure 3 we show the prominence under study observed by SOHO/EIT in four EIT lines: Fe IX/X 171 Å, Fe XII 195 Å, Fe XV 284 Å, and He II 304 Å. In the He II line the prominence appears bright. Although, according to Delaboudinière *et al.* (1995), this line is supposed to be formed in the transition region at temperatures around 80 000 K the observed brightness results mainly from resonance scattering of chromospheric radiation in cooler parts of the prominence (Labrosse and Gouttebroze, 2001, 2004). In the other EIT lines the structure corresponding to He II 304 Å emission is not visible but a rather extended brightness depression can be clearly seen. At the wavelengths of the three iron lines the opacity will be comparable to that of the Hα line; see Anzer and Heinzel (2005). Therefore a certain amount of absorption should be present under these circumstances. The fact that the darkest prominence structure does not show up in these lines then implies that the blocking actually has to be the dominant mechanism and the absorption is too faint to be detected.

4.3. Dark Structures in Soft X-Rays

In soft X-rays a brightness depression in the corona was noticed by Batchelor and Schmahl (1994), who show several examples of coronal SXR darkenings detected by the soft X-ray telescope (SXT) onboard *Yohkoh*. Although these examples are not very convincing (the SXR corona is usually very inhomogeneous), the dark features were interpreted by these authors as being due to the continuum absorption in the X-ray region. But as we shall show in the following this interpretation does not seem acceptable.

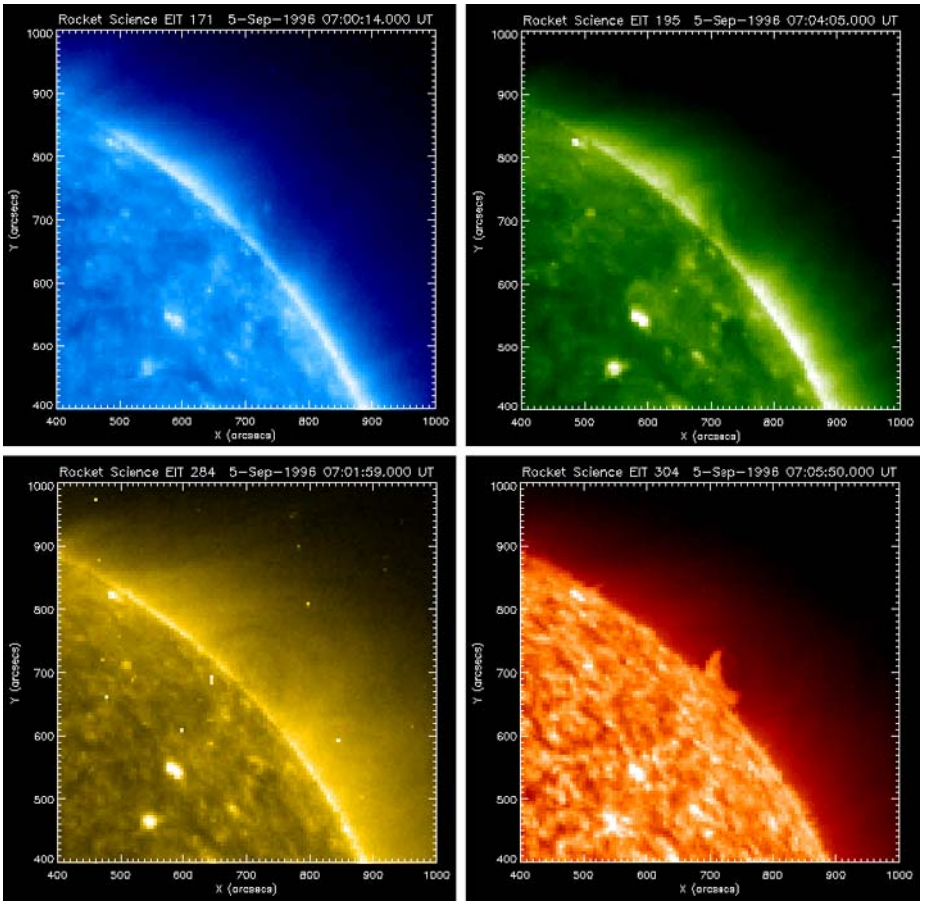

Figure 3 The prominence under study observed by SOHO/EIT on 5 September 1996, in 171 Å (upper left), 195 Å (upper right), 284 Å (lower left), and 304 Å (lower right).

The region around the 5 September 1996, prominence was also observed by *Yohkoh*/SXT and thus we are able to compare the SXR features with the aforementioned UV and EUV structures seen by SOHO. In Figure 4 (upper part) we show again the SOHO/EIT image in the He II 304 Å line (left), which can be compared with an SXT image (right) taken in the Al.1 filter about one hour later. We see clearly an extended dark feature, but it resembles more the brightness depression seen previously in hot EIT coronal lines, rather than narrower "cool" structure. To demonstrate this better, we show in Figure 4 (lower part) the SXT image overlaid by contours that correspond to He II 304 Å line (left) and Fe 195 Å line (right).

Our calculations of the absorption cross section for soft X-rays at 50 Å show very convincingly that the observed darkening in this wavelength range cannot be due to absorption. Therefore it has to be produced by the effect of *emissivity blocking*.

4.4. Modeling of the 5 September 1996, Prominence

In this section we describe briefly how our modeling procedure works. For this demonstration we use the EIT data from SOHO and the SXT data from *Yohkoh*. A closer look at the

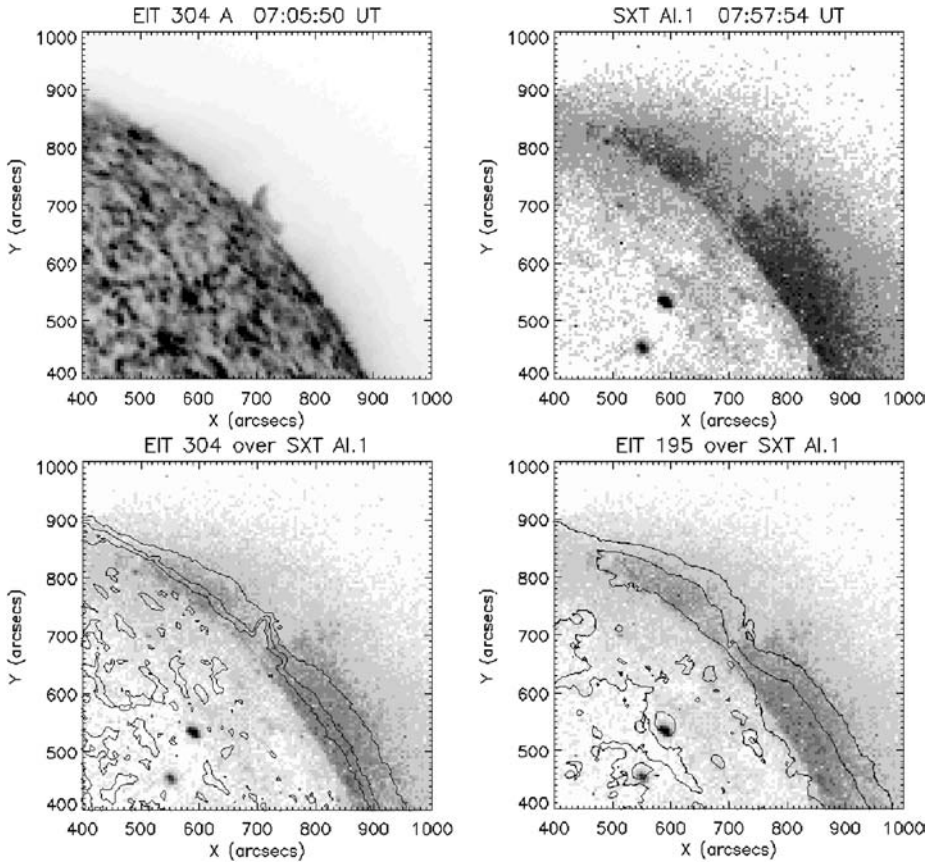

Figure 4 Two upper images: SOHO/EIT image of the prominence in 304 Å (left) and the *Yohkoh*/SXT image of the same region (right); both images here are negatives. Two lower images: SOHO/EIT image in 304 Å (left) and 195 Å (right) overlaid as contours over the *Yohkoh*/SXT image. The structure in the middle seen in 304 Å fits well into the SXR emission gap.

EIT data indicates that the best results are obtained with the Fe XII line at 195 Å. For this line we made several horizontal cuts at different heights and estimated the ratio I/I_c for each cut. We then took the average of all these ratios and found

$$I/I_c = 0.56.$$

The SXT data are much noisier; therefore it was necessary to average the count rates over several pixels in the vertical direction. On this basis we were able to determine a useful value of ratio of the count rates of

$$I/I_c = 0.68.$$

Because for the X-rays τ is approximately zero we get from the X-ray data and our Equation (2) an estimate for the blocking length L of

$$L/L_0 = 0.32.$$

With this value for L/L_0 and the ratio $I/I_c = 0.56$ for the 195 Å line we can then calculate the optical depth at this wavelength:

$$\tau_{195} = 0.43.$$

These two quantities can be used to specify the physical model for the prominence. With $L_0 = 420\,000$ km the blocking length amounts to $L = 135\,000$ km. (Note that this path may contain, apart from the cool prominence, also part of a coronal void around the prominence, which acts on the emissivity blocking in the same way and thus cannot be distinguished from the prominence itself.) For the optical depth in Hα we estimate $\tau_{H\alpha} = 0.3$, using the results of Anzer and Heinzel (2005). By taking some typical value for the effective absorption cross section at 195 Å we also can calculate the hydrogen column density along the line of sight, obtaining $N_H = 2.7 \times 10^{18}$ cm^{-2}. One sees that all these values are quite reasonable, which gives us confidence into the reliability of this new method. In fact, this method can be directly compared with a similar one used by Heinzel, Dammsch, and Anzer (in preparation) for the SUMER data. Although we did not directly use the 195 Å line together with Fe XII (replacing the X-ray data), using the Mg X line as a strong absorption line we derived the expected τ for 195 Å. This is summarized in Table 1; the value of 0.37 for the 195 Å line is quite comparable to the 0.43 obtained when one derives the blocking from X-ray data. This actually should be the case because the coronal plasma observed by SXT with the Al.1 filter and by SUMER at the Fe XII line is at the same temperature and thus has a similar emissivity distribution.

To estimate the accuracy of our modeling we note that the ratios of I/I_c in both the iron line and in X-rays are typically uncertain by about 10%. Using now lower and upper limits of these ratios we find that L/L_0 lies in the range 0.25 – 0.39. With these values we then get for τ_{195} a range of 0 to approximately 1. This indicates that the blocking length is quite well determined whereas τ is more uncertain. The new *Hinode* data should allow a more accurate determination of these prominence parameters.

5. Prominence Observations with *Hinode* Instruments

The new Japanese satellite *Hinode* (formerly named Solar-B) was successfully launched on 23 September 2006. It will provide new and better opportunities to observe solar prominences. This satellite contains an optical telescope (SOT), an EUV imaging spectrometer (EIS), and an X-ray telescope (XRT). For our discussion here, only the EIS and XRT instruments are important. EIS observes in two wavelength regions, 170 – 210 Å and 250 – 290 Å. Its sensitivity is about a factor 10 higher than that of SOHO/EIT. The pixel size is 1″ and the spectral resolution is 2.23 mÅ per pixel. There are two slits of 1″ × 512″ and 2″ × 512″ and two slot modes with 40″ × 512″ and 250″ × 512″. The two spectral windows contain the iron lines at 171, 195, and 284 Å used by EIT. The XRT instrument has nine filters, which are sensitive in the temperature range given by $\log(T) = 6.1 - 7.5$. The pixel size is 1″ × 1″ and the total field of view is 2018″ × 2018″. The resolution of the X-ray telescope is considerably higher than that of *Yohkoh*/SXT. But since the only X-ray signature of prominences on the limb is the *emissivity blocking* effect, which requires rather large spatial structures, we do not expect to observe any very fine structures in X-rays. Nevertheless, the high resolution is still useful as it allows averaging over many pixels, which can reduce the noise considerably. As has been shown in the previous sections a combined observational program in some selected EUV lines together with X-ray observations will be very useful for the investigation of the physics of solar prominences.

Using some coordinated observations with the *Hinode*/XRT instrument and SOHO/SUMER-CDS we can study both the central parts of prominences that are well visible in Hα as well as the so-called EUV extensions (Heinzel, Schmieder, and Tziotziou, 2001; Schwartz *et al.*, 2004; Anzer and Heinzel, 2005). The latter ones retain a significant opacity in the H I Lyman continuum at wavelengths around 600 Å. (Note that the Mg X line observed by SUMER and CDS lies at 625 Å.) However, at shorter wavelengths where the continua of He I and also He II become important the opacity of these EUV extensions becomes very low and therefore only the emissivity blocking is operating. But in the Hα parts of the prominence the EUV opacity for the spectral windows of EIS are typically of the same magnitude as the one in Hα (see Anzer and Heinzel, 2005) and should therefore have an important effect.

6. Discussion

Based upon our investigations with the SOHO/EIT and *Yohkoh*/SXT instruments we suggest new observations using EIS and XRT on the recently launched satellite *Hinode*. From the intensity measurements in the EUV lines and in the X-ray continuum one can calculate the absorption effect and the emissivity blocking. These measurements will give us the thickness of the prominence and the column density along the line of sight. If in addition some lines both above and below the edge of the He II continuum at 228 Å are considered we can also calculate the degree of helium ionization. All these quantities can then be used to construct physically realistic prominence models.

The observational program could be extended further when SOHO/SUMER-CDS data are included. Such a coordinated program would allow us to study some lines around 600 Å, which have a large enough opacity to show the EUV extensions. In this case also the physics of the extensions can be better understood.

Acknowledgements U.A. thanks the Astronomical Institute in Ondřejov for the hospitality and for financial support. Part of this work was done when P.H. and F.F. were visiting the MPA in Garching. This work was supported by ESA-PECS Project No. 98030 and by the research project AV0Z10030501. We also thank the referee for useful comments.

References

Anzer, U., Heinzel, P.: 2003, *Astron. Astrophys.* **404**, 1139.
Anzer, U., Heinzel, P.: 2005, *Astrophys. J.* **622**, 714.
Batchelor, D.A., Schmahl, E.J.: 1994, In: Hunt, J.J. (ed.) *Proceedings of 3rd SOHO Workshop, ESA SP-373*, 203.
Del Zanna, G., Chiuderi, D.F., Parenti, S.: 2004, *Astron. Astrophys.* **420**, 307.
Delaboudinière, J.-P. *et al.*: 1995, *Solar Phys.* **162**, 291.
Engvold, O., Kjeldseth-Moe, O., Bartoe, J.-D., Brueckner, G.E.: 1987, In: Battrick, B., Rolfe, E.J. (eds.) *Small-Scale Plasma Processes, ESA SP-275*, 21.
Feldman, U., Dammasch, I., Wilhelm, K., Lemaire, P., Hassler, D.M.: 2003, In: Battrick, B. (ed.) *Images of the Solar Upper Atmosphere from SUMER on SOHO, ESA SP-1274*.
Foukal, P.: 1981, *Astrophys. J.* **245**, 304.
Heinzel, P., Schmieder, B., Tziotziou, K.: 2001, *Astrophys. J.* **561**, L223.
Heinzel, P., Anzer, U., Schmieder, B.: 2003, *Solar Phys.* **216**, 159.
Heinzel, P., Fárnik, F., Anzer, U., Dammasch, I.: 2007, In: Shibata, K., Nagata, S., Sakurai, T. (eds.) *New Solar Physics with Solar-B Mission, Astron. Soc. Pac. Conf. Ser.* **369**, in press.
Kucera, T., Andretta, V., Poland, A.I.: 1998, *Solar Phys.* **183**, 107.
Labrosse, N., Gouttebroze, P.: 2001, *Astron. Astrophys.* **380**, 323.
Labrosse, N., Gouttebroze, P.: 2004, *Astrophys. J.* **617**, 614.
Rumph, T., Bowyer, S., Vennes, S.: 1994, *Astron. J.* **107**, 2108.
Schwartz, P., Heinzel, P., Anzer, U., Schmieder, B.: 2004, *Astron. Astrophys.* **421**, 323.